NUSC Reprint Report 6640
15 July 1987

# An Analysis of Developing Turbulent Flow Between a Moving Cylinder and a Concentric Tube

D. A. Kotlow
Launcher and Missile Systems Department

F. M. White
University of Rhode Island





Naval Underwater Systems Center
Newport, Rhode Island / New London, Connecticut



*Reprint of a paper presented at the ASME / AIAA 4th Joint Fluid Mechanics, Plasma Dynamics, and Lasers Conference, Atlanta, GA, May 1986.*

# AN ANALYSIS OF DEVELOPING TURBULENT FLOW BETWEEN A MOVING CYLINDER AND A CONCENTRIC TUBE

D. A. Kotlow
Naval Underwater Systems Center
Newport, Rhode Island 02841

F. M. White
University of Rhode Island
Kingston, Rhode Island 02881

## Abstract

A numerical analysis is made of developing and developed turbulent flow in the annular region between a cylinder moving at constant velocity within a fixed concentric tube. Turbulent shear is modeled by eddy viscosity, and a uniform velocity is assumed at the entrance to the annular region. The computations extend and modify the method of Sud and Chaddock (1981) to arbitrary Reynolds numbers and radius ratios. Approximate formulas are given for both developing and developed values of pressure drop, shear stress on the inner and outer walls, and total cylinder drag.

## Nomenclature

| | | |
|---|---|---|
| $a$ | = | $r_{mt}/r_i$ |
| $b$ | = | $r_o/r_i$ |
| $C$ | = | parameter defined in Eq. (11) |
| $D_h$ | = | hydraulic diamater, $2(r_o-r_i)$ |
| $f$ | = | friction factor, Eq. (20) |
| $F$ | = | drag force, Eq. (14) |
| $L^*$ | = | entrance length, Fig. 7 |
| $n$ | = | eddy viscosity parameter, Table 1 |
| $p$ | = | pressure |
| $r$ | = | radial coordinate |
| $r_{mt}$ | = | radius of maximum velocity, Fig. 2 |
| $Re_v$ | = | $U_v r_i/\nu$ |
| $Re_b$ | = | $U_b D_h/\nu$ |
| $u$ | = | axial velocity |
| $U_b$ | = | average annular velocity, Eq. (1) |
| $U_v$ | = | inner cylinder or vehicle velocity |
| $U$ | = | inviscid core velocity, Fig. 2 |
| $v^*$ | = | friction velocity, $(\tau_w/\rho)^{1/2}$ |
| $x$ | = | axial coordinate |
| $y$ | = | coordinate normal to wall, Fig.2 |
| $y^+_\ell$ | = | eddy viscosity crossover point, Table 1 |
| $\delta$ | = | boundary layer thickness |
| $\rho$ | = | density |
| $\nu$ | = | kinematic viscosity |
| $\tau$ | = | shear stress |
| $\tau^*$ | = | $2\tau/\rho U_v^2$ |

Superscript

| | | |
|---|---|---|
| + | = | law-of-the-wall coordinates, Eq. (4) |

Subscripts

| | | |
|---|---|---|
| i | = | inner wall |
| o | = | outer wall |
| w | = | either wall |
| fd | = | fully developed |
| $\delta$ | = | inviscid core value |
| E | = | in the entrance region |

## Introduction

The problem of turbulent flow in a concentric annulus has been of interest for at least eight decades, beginning with the experimental results of Becker (1907). Numerous papers have treated the problem of pressure-driven flow between fixed cylinders. For fully developed flow, the eddy viscosity theory of Quarmby(1968) is in good agreement with his experimental results (Quarmby 1966). For both laminar and turbulent flow in a fixed annulus, the point of maximum axial velocity $r_{mt}$ is closer to the inner radius (Lawn and Elliot 1972).

Developing annular flow is less well documented, but an integral analysis by Wilson and Medwell (1971) shows a development length for turbulent flow of about ten hydraulic diameters for Reynolds numbers from $10^4$ to $3\times10^5$ and radius ratios from 1.25 to 5.0. Their results agree reasonably well with data by Okiishi and Serovy (1967).

The problem under study here is the annular flow driven by uniform axial motion of the inner cylinder, which simulates the motion caused by vehicles travelling in tubes or by the launching of torpedoes or cylindrical buoys. Experimental data on vehicles in tubes are summarized by Davidson (1974), and theoretical results are given in the book by Hammit (1973). Implicit in the analysis of the annular flow induced by a moving cylinder is the assumption that the volume swept out by the vehicle passes through the annulus to fill the void behind the vehicle, as in Figure 1. This simulates a very long outer tube, whereas in a short tube the inlet and outlet can serve as a source and sink of fluid, with less volume passing through the annulus. The only detailed analysis of the flow shown in Figure 1 is given by Sud and Chaddock (1981), for both developing and developed flows. After presenting a general analytical technique, Sud and Chaddock give computed results for only a single case, $r_o$ = 8 ft (2.44 m), $r_i$ = 6 ft (1.83 m), and $U_v$ = 200 ft/s (61 m/s), at two air densities (Reynolds numbers).

It is the purpose of the present paper to extend the analysis of Sud and Chaddock to arbitrary radius ratios and Reynolds numbers, for both developing and developed flow. The developed flow analysis is identical to Sud and Chaddock. For developing flow, corrections are made to their analysis, as it is felt that Sud and Chaddock's results in the entrance region are somewhat inaccurate.

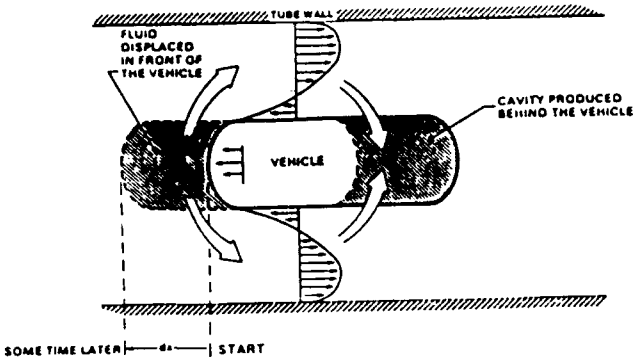


Figure 1. If a vehicle moves through a long tube, the volume swept out passes through the annulus.

## Fully Developed Flow

The geometry of the flow is shown in Figure 2. With coordinates fixed to the vehicle, both the upstream fluid and the outer tube wall appear to move at vehicle velocity $U_v$. Based on the displacement concept of Figure 1, the incompressible continuity relation requires that the average velocity $U_b$ in the annular region be related to vehicle velocity by

$$U_b = U_v b^2/(b^2-1) \qquad (1)$$

where $b = r_o/r_i$ is the principal geometric parameter in the analysis.

In the fully developed region, $u = u(r)$ only, and the flow may be divided into an inner region "i" and an outer region "o", separated by the point of maximum velocity, $r_{mt}$. Since there is no acceleration in the developed region, a momentum balance shows that the inner and outer wall shear stresses are related by

$$\frac{\tau_o}{\tau_i} = \frac{b^2 - a^2}{b(a^2-1)} \qquad (2)$$

where $a = r_{mt}/r_i$.

There are two characteristic Reynolds numbers: for the vehicle motion, $Re_v = U_v r_i/\nu$, and for the annular flow, $Re_b = U_b D_h/\nu$, where $D_h = 2(r_o-r_i)$ is the hydraulic diameter. The two are related by geometry and continuity:

$$Re_b = 2b^2 Re_v/(b+1) \qquad (3)$$

The analysis follows Sud and Chaddock (1981). Both the inner and outer regions are divided into two computational regions as in Fig. 2: (1) the sublayer, and (2) the turbulent core. The flow is assumed steady, incompressible, and turbulent, with impermeable walls. The variables are non-dimensionalized in law-of-the-wall fashion:

$$u^+ = u/v^* \; ; \quad y^+ = yv^*/\nu \; , \; v^* = (\tau_w/\rho)^{1/2} \qquad (4)$$

The sublayer, $0 \le y \le y_\ell$, is modeled with Deissler's eddy viscosity formulation:

$$\frac{du^+}{dy^+} = \frac{\tau/\tau_w}{1 + n^2 u^+ y^+ [1 - \exp(-n^2 u^+ y^+)]} \qquad (5)$$

The turbulent core, $y_\ell \le y \le y_{mt}$, is modeled with Karman's similarity hypothesis for eddy viscosity:

$$\frac{d^2u^+}{dy^{+2}} = \frac{\kappa\,(du^+/dy^+)^2}{(\tau/\tau_w - du^+/dy^+)^{1/2}} \; , \quad \kappa = 0.36 \qquad (6)$$

In both cases, the local shear stress is related to local radius through a momentum balance:

$$\frac{\tau}{\tau_w} = \frac{r_w\,(r^2 - r_{mt}^2)}{r\,(r_w^2 - r_{mt}^2)} \qquad (7)$$

At high Reynolds numbers, Deissler's damping parameter $n^2$ equals 0.0154 with the cross-over point $y^+_\ell = 15.0$. At lower Reynolds numbers, values of $n^2$ and $y^+_\ell$ were taken from a graph given by Quarmby (1968). Some typical values are given here in Table 1. These values are not thought to be especially accurate but are retained for comparison to the analyses of Quarmby (1968) and Sud and Chaddock (1981).

Equations (5,6,7) are a set of differential equations to solve for the velocity profiles $u_i$ and $u_o$ in the inner and outer regions. From Fig. 2, the boundary conditions are

$$\begin{aligned} y_i &= 0 \; ; \quad u_i = 0 \\ y_o &= 0 \; ; \quad u_o = U_v \end{aligned} \qquad (8)$$

The equations are solved by an iterative technique similar to Sud and Chaddock but modified by Kotlow (1985). One begins by guessing $\tau_o$ and a (or $r_{mt}$), whence $\tau_i$ can be computed and the velocity profiles $u_i$ and $u_o$ computed by numerical (Runge-Kutta) integration of Eqs. (5,6,7). The value of $\tau_o$ is gradually adjusted and the integrations repeated until the core velocity $U_{\delta o}$ exceeds $U_b$. If the two profiles do not meet at $r_{mt}$ with $U_{\delta i} = U_{\delta o}$ then a new value of a is computed from the relation

$$a = \left(\frac{b(1 + ba^2)}{b + a^2}\right)^{1/2}, \quad \alpha = U^+_{\delta o}/U^+_{\delta i} \qquad (9)$$

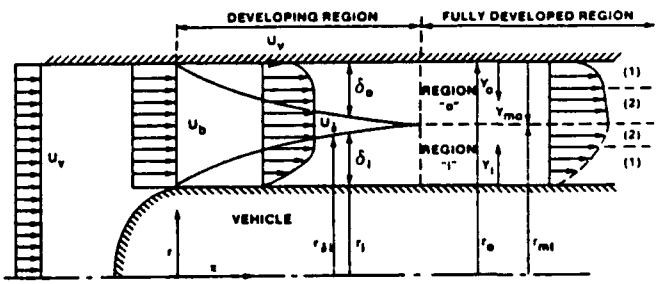


Figure 2. Velocity and boundary layer development of fluid in the annular region (modified from Sud and Chaddock 1981).

The entire process is then repeated until the value of a converges. The profiles are then integrated to determine the average velocity $U_b$, which is compared with Eq. (1). If there is a mismatch, the value of $\tau_o$ is again adjusted and the entire double-iteration process is repeated until final convergence. With the profiles known, the pressure drop, friction factor, and other parameters are computed.

Table 1 Eddy Viscosity Parameters at Low Reynolds Numbers

| $y^+_{mt}$ | $n^2$ | $Re_b$ | $y^+_\ell$ |
|---|---|---|---|
| 100 | 0.0074 | 10000 | 26.7 |
| 200 | 0.0127 | 20000 | 20.0 |
| 300 | 0.0142 | 30000 | 17.6 |
| 400 | 0.0150 | 40000 | 16.2 |
| $\geq$ 500 | 0.0154 | $\geq$ 50000 | 15.0 |

Using the above procedure, Kotlow (1985) has tabulated fully-developed flow parameters for a range of $Re_v = 10^4$-$10^8$ and radius ratios b = 1.01-2.0. The fully-developed friction factor is defined by

$$f_{fd} = \frac{(-dp/dx)\, D_h}{\frac{1}{2}\rho U_v^2} = \frac{8(r_o\tau_o + r_i\tau_i)}{(r_o+r_i)\,\rho U_v^2} \qquad (10)$$

Values of $f_{fd}$ are plotted in Fig. 3 from the above theory. The pressure drop is very large at small values of b due to the high bulk velocity in the annulus, Eq. (1). The curves in Fig. 3 can be collapsed approximately into a Moody-chart type of curve by scaling Reynolds number and pressure drop with $U_b$ rather than $U_v$. Note the agreement in Fig. 3 with the two computed points of Sud and Chaddock (1981) for b = 1.33.

The computed curves in Fig. 3 may be fit to the following algebraic formula with good accuracy:

$$f_{fd} = C^2\,[0.001 + 2.8/(\log_{10}Re^*)^{3.1}], \qquad (11)$$

where $C = \dfrac{b^2+1}{2(b^2-1)}$ and $Re^* = \dfrac{2b^2}{b+1}\,Re_v$

The error when compared to Fig. 3 is about ±3% in the range $Re_v = 10^5$-$10^8$.

Kotlow (1985) also tabulates values of the dimensionless inner and outer wall shear stresses. The inner stress is the higher and, for fully-developed flow, these stresses may be estimated by the following curve-fit formulas:

$$\tau_i^* = \beta\tau_o^*, \quad \beta = 1.005\, b^{1.543+0.2195\,\log_{10}Re_v} \qquad (12)$$

$$\tau_o^* = \frac{f_{fd}(b+1)}{4(b+\beta)} \qquad (13)$$

where $f_{fd}$ is to be estimated from Eq. (11). Equations (12) and (13) have an accuracy of about ±4% over the range $Re_v = 10^5$-$10^8$ and b = 1.01-2.0.

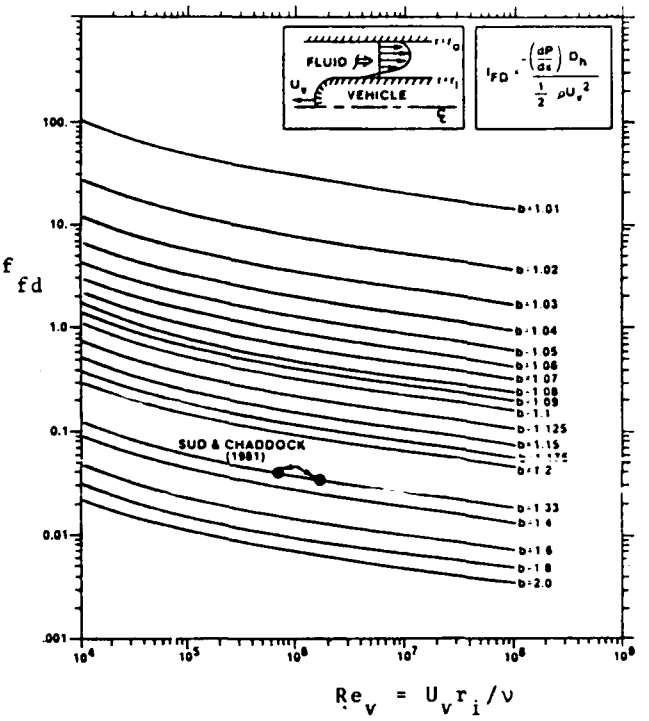


Figure 3. Theoretical fully-developed friction factors in the annular region.

In the fully-developed region, the drag experienced by the vehicle would be a combination of pressure difference and inner wall shear. For a cylinder of length L, the drag would be

$$F_{fd} = \pi r_i L\left(2\tau_i - r_i\frac{dp}{dx}\right) \qquad (14)$$

This estimate must be supplemented by values of nose drag, wake drag, and the increased pressure drop and shear in the developing region (Davidson 1974).

Finally, the moving inner cylinder causes the point of maximum velocity to shift toward the outer wall, unlike the fixed annulus case. This position is shown in Fig. 4 and becomes closer to the outer wall as Reynolds number and radius ratio increase. The same qualitative effect occurs for laminar flow.

## Developing Flow in the Entrance

Experimentally, the pressure and shear stress in the entrance region are dependent upon exact entrance conditions: sharp-edged, rounded-edge, bellmouth, etc. Some experimental results for a fixed annulus are given by Okiishi and Serovy (1967), Rothfus et al. (1955), and Olson and Sparrow (1963). These results are discussed by Kotlow (1985).

The present analysis follows Sud and Chaddock (1981) by assuming that the entrance velocity profile is uniform, $u = U_v$, as in Fig. 2. Boundary layers $\delta_i$ and $\delta_o$ grow on the walls until they meet at $x = L^*$, the entrance length. At any x, the core velocity $U_\delta(x)$ is assumed uniform.

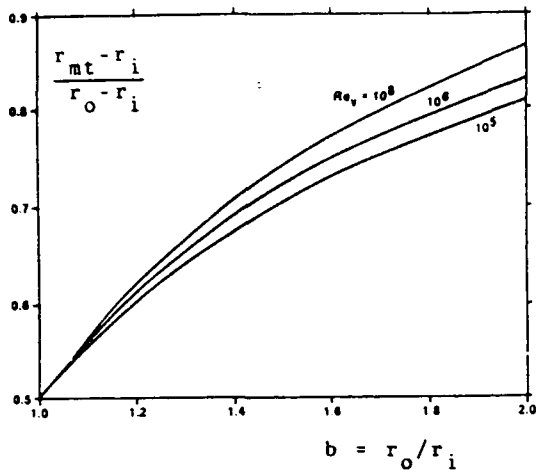


Figure 4. Computed position of maximum velocity in the annulus for fully-developed flow.

At any given x, variables $u^+$ and $y^+$ are scaled with local shears $\tau_i(x)$ and $\tau_o(x)$ and the boundary layer profiles $u_i$ and $u_o$ computed by integration of Eqs. (5) and (6). Since $\tau(y)$ is not known in the developing region, the linear profile assumption of Wilson and Medwell (1971) was adopted

$$\tau(y) = \tau_w(1 - y/\delta) \qquad (15)$$

for both the inner and outer regions.

The study began by repeating the computations of Sud and Chaddock (1981) for the special case given in their Figures 3 and 4. Only qualitative agreement was obtained, and the computations indicated that local mass and momentum balances were not accurately satisfied. The discrepancy, if any, was difficult to analyze, for Sud and Chaddock used the transformation technique of Wilson and Medwell (1971), resulting in a double integral with extremely complex arguments. In any case, the Sud and Chaddock approach was abandoned and instead a local mass and momentum balance was used to compute incremental changes in velocity, pressure, and shear. Developing flow was thus computed for the ranges $Re_v = 10^5$-$10^7$ and $b = 1.01$-$2.0$.

A momentum balance over a short distance $\Delta x$ of inner boundary layer gives Eq. (20) of Sud and Chaddock (1979):

$$\frac{\Delta p}{2}\left[(r_i+\delta_i)^2 - r_i^2\right] + \bar{\tau}_i r_i \Delta x =$$

$$= U_\delta \Delta\left[\int_{r_i}^{r_i+\delta_i} \rho u_i r\, dr\right] - \Delta\left[\int_{r_i}^{r_i+\delta_i} \rho u_i^2 r\, dr\right] \qquad (16)$$

where $\bar{\tau}_i$ is the average inner wall shear. An exactly similar relation holds for the outer boundary layer.

A momentum balance of the entire annular flow gives

$$\frac{\Delta p}{2\rho}(r_o^2 - r_i^2) + \frac{\Delta x}{2\rho}(r_i\bar{\tau}_i + r_o\bar{\tau}_o) = \Delta I, \qquad (17)$$

where $I = \int_{r_i}^{r_i+\delta_i} u_i^2 r\, dr + \int_{r_i+\delta_i}^{r_o-\delta_o} U_\delta^2 r\, dr + \int_{r_o-\delta_o}^{r_o} u_o^2 r\, dr$

Using values of $(\tau_i, \tau_o, \delta_o)$ from the previous step and estimating a new value for $\delta_i$, the velocities $u_i$ and $u_o$ were computed from Eqs. (5,6,15) for the next step $x+\Delta x$. The integrated average of the velocity profile was compared with $U_b$ from Eq. (1) and $\tau_i$ was adjusted until mass balance was achieved. At the same time, $\tau_o$ was continually adjusted within an inner loop to meet the condition $U_{\delta i} = U_{\delta o}$. The three momentum balances were used to estimate $\Delta x$ and $\delta_o$ was adjusted and the procedure repeated iteratively until the location of $u_o$ matched that of $u_i$.

The inviscid-core Bernoulli relation, $dp = -\rho U_\delta dU_\delta$, was omitted in favor of simultaneously balancing the inner, outer, and overall momentum relations. Use of the Bernoulli relation seemed to induce numerical instabilities or errors, such that the pressure gradient or wall shears fell below their fully-developed values (Kotlow 1985). Several discrepancies of this type are seen in the tabulated results of Sud and Chaddock (1979), who used the Bernoulli relation.

A direct comparison was made with the special case computed by Sud and Chaddock (1979,1981): $r_i = 1.83$ m, $r_o = 2.44$ m, $U_v = 61$ m/s, for air at 37°C and 0.25 atm. The results are shown in Fig. 5 for the local pressure drop. The two results are similar, but the present computations are smoother and perhaps slightly more accurate.

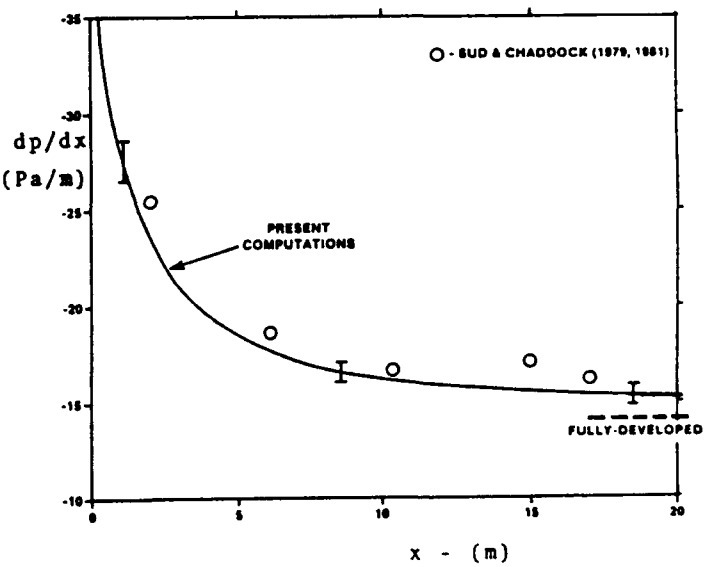


Figure 5. Comparison with the special case computed by Sud and Chaddock. (Bars denote numerical uncertainty.)

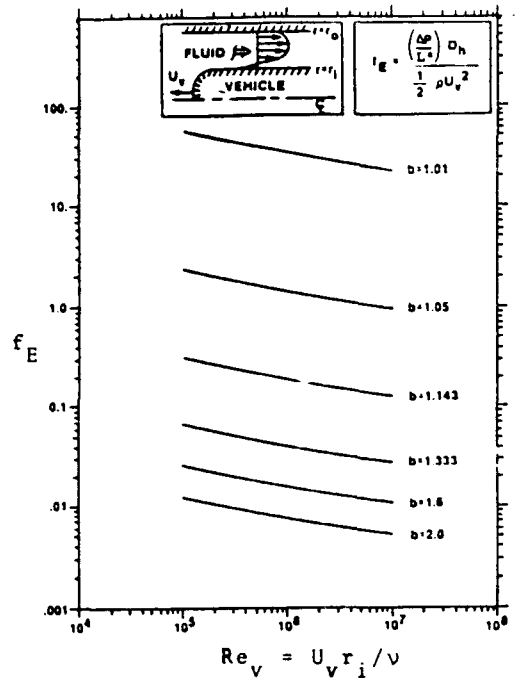


Figure 6. Computed overall friction factors in the developing region.

Figure 6 shows the computed friction factors in the entrance region, defined as the dimensionless pressure drop between x=0 and x=L*, the entrance length. These values everywhere exceed the fully-developed friction factors from Fig. 3. They may be curve-fit by the relation

$$f_E \doteq f_{fd} + 0.032\, C^2\, Re_v^{-0.2} \qquad (18)$$

where $f_{fd}$ is estimated from Fig. 3 or Eq. (11). The overall accuracy is ±3% in the range $Re_v = 10^5$-$10^7$ and b = 1.01-2.0.

Similarly, the integrated average inner-wall shear stress over the entrance length L* may be curve-fit by

$$\bar{\tau}_i^* \doteq \tau_{i,fd}^* + 0.0068\, C^2\, b^{0.559}\, Re_v^{-0.205} \qquad (19)$$

where $\tau^* = 2\tau/\rho U_v^2$ and the fully-developed value is estimated from Eqs. (12) and (13). The overall accuracy of Eq. (19) is ±3.5% for $Re_v = 10^5$-$10^7$ and b = 1.01-2.0.

Finally, the computed entrance lengths L* are shown in Fig. 7 as a function of Reynolds number and radius ratio. These results are larger than the integral estimates for a fixed annulus flow by Wilson and Medwell (1971). They may be curve-fit by the formula

$$L^*/D_h \doteq (4.17 \log_{10} Re_v - 7.875)\, b^{1.1} \qquad (20)$$

with an overall accuracy of ±4%.

If the cylinder is of length $L_v$ greater than L*, its overall drag coefficient is the sum of an entrance drag plus fully-developed drag on the aft portion ($L_v$-L*):

$$C_D = \frac{L^*}{D_h}\left(4(b-1)\bar{\tau}_{i,E}^* + f_E\right) + \frac{(L_v - L^*)}{D_h}\left(4(b-1)\tau_{i,fd}^* + f_{fd}\right) \qquad (21)$$

Each of the parameters in this expression may be estimated from the previous curve-fit formulas (11) to (20). The overall accuracy for the drag is ±6%.

Although not shown here, the inner and outer velocity profiles, when plotted in law-of-the-wall coordinates, $u^+$ versus $y^+$ and $(u^+ - U^+)$ versus $y^+$, were in excellent agreement with the traditional linear sublayer and logarithmic layer formulas. This was true for all $Re_v$ and b computed, in both the developing and developed regions.

However, in their fixed-annulus experiment, Lawn and Elliot (1972) report that inner-wall velocity data failed to correlate with the law-of-the-wall for their largest b = 11.36. Such large radius ratios were not computed here.

## Conclusions

The use of straightforward eddy viscosity models and integral mass and momentum balances leads to a complete set of analytical results for the turbulent annular flow between a fixed outer cylinder and a moving concentric inner cylinder. The results are in good agreement with the two special cases computed earlier by Sud and Chaddock (1979,1981) and with the data of Davidson (1974).

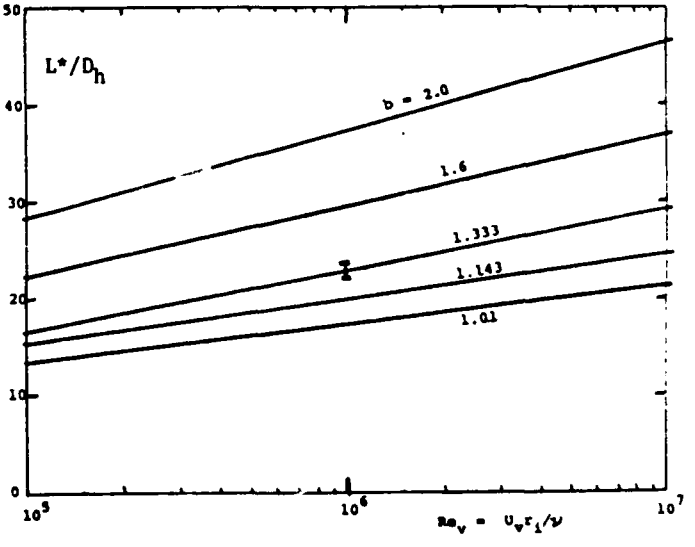


Figure 7. Computed entrance lengths for various radius ratios.

The pressure drop and wall shear stresses in both the developing and fully-developed regions are smoothly varying functions of Reynolds number and radius ratio. They may be fit to simple algebraic correlations which have an accuracy of about five percent. The friction factor in the fully-developed region may be directly related by scaling factors to the ordinary Moody-chart friction factor for circular pipe flow. Development lengths vary from ten to forty hydraulic diameters, increasing slowly with both Reynolds number and radius ratio.

## Acknowledgement

The support of the Naval Underwater Systems Center, Newport, R.I., under Independent Research and Independent Exploratory Development Project A43126, is acknowledged.

## References

Becker, E., 1907, "Stromungsvorgange in Ringformigen Spalten (Labyrinth-Dichugen)", Zeit. V.D.I., Vol. 51, pp. 1133-1141.

Davidson, J.V., 1974, "Aerodynamic Drag of Tube Vehicles", M.S. Thesis, Duke Univ., Durham, N.C.

Hammit, A.G., 1973, The Aerodynamics of High Speed Ground Transportation, Western Periodicals Co.

Kotlow, D.A., 1985, "Aerodynamic Drag of Cylindrical Vehicles Moving Concentrically within Long Tubes", M.S. Thesis, Univ. of Rhode Island, Kingston, RI.

Lawn, C.J., and Elliot, C.J., 1972, "Fully Developed Turbulent Flow through Concentric Annuli", J. Mechanical Engineering Science, Vol.14, June, pp. 195-204.

Okiishi, T.H., and Serovy, G.K., 1967, "An Experimental Study of the Turbulent-Flow Boundary-Layer Development in Smooth Annuli", J. Basic Engineering, Vol. 89, Dec., pp. 823-836.

Olson, R.M., and Sparrow, E.M., 1963, "Measurements of Turbulent Flow Development in Tubes and Annuli with Square or Rounded Entrances", A.I.Ch.E. Journal, Nov., pp. 766-770.

Quarmby, A., 1966, "An Experimental Study of Turbulent Flow through Concentric Annuli", Int. J. of Mechanical Science, Vol. 9, April, pp. 205-221.

Quarmby, A., 1968, "An Analysis of Turbulent Flow in Concentric Annuli", Appl. Scientific Research, Vol. 19, July, pp. 250-293.

Rothfus, R.R., Monrad, C.C., Sikchi, R.G., and Heideger, W.J. (1955), "Isothermal Skin Friction in Flow through Annular Sections", Industrial and Engineering Chemistry, Engineering Design and Process Development, pp. 913-918.

Sud, I., and Chaddock, J.B., 1979, "Drag Calculations for Vehicles in Tubes from Turbulent Flow Theory", ASME Symposium on Aerodynamics of Transportation, T. Morel and C. Dalton, ed., June 18-20, Niagara Falls, NY, pp. 165-176.

Sud, I., and Chaddock, J.B., 1981, "Drag Calculations for Vehicles in Very Long Tubes from Turbulent Flow Theory", ASME JOURNAL OF FLUIDS ENGINEERING, Vol. 103, June, pp. 361-366.

Tomotika, S., Tamada, K., and Saito, T., 1940, "Application of the Similarity Theory of Turbulence to the Flow through a Straight Pipe of Annular Cross-Section", Rept. Aero. Res. Inst. Tokyo Imp. Univ., Vol. 15, p. 29.

Wilson, N.W., and Medwell, J.O., 1971, "An Analysis of the Developing Turbulent Hydrodynamic and Thermal Boundary Layers in an Internally Heated Annulus", J. Heat Transfer, Vol. 64, Feb., pp. 25-32.